Underwater Wireless Laser-Based Communications Using Optical Phased Array Antennas

Ali Derakhshandeh, Stephan Pachnicke, *Senior Member, IEEE*, and Peter A. Hoeher, *Fellow, IEEE*

***Abstract*—An underwater optical wireless communication system concept based on optical phased array antennas is presented. With this optical phased array, a laser beam can be electronically steered to adjust not only the azimuth and elevation angles, but also the beamwidth.The proposed concept simplifies pointing and acquisition challenges between non-aligned transceivers. The performance (in terms of the trade-off between achievable range, bit error rate, and data rate) is explored for different numbers of antenna elements and water types. Also, a suitable scanning method is suggested.**

***Index Terms*—Laser applications, optical phased array, pointing and acquisition, underwater optical wireless communication.**

I. Introduction

THE significant increase in underwater missions and the growing capability of underwater sensors to gather information necessitate higher data rate communications. On the other hand, the collaboration between underwater vehicles and/or fixed sensors to support a vast variety of tasks relies heavily on the presence of high-capacity communication links. Compared to alternative underwater wireless communication methods that use acoustic waves, radio waves, magnetic fields, or electric fields, underwater wireless optical communication (UOWC) offers the highest achievable data rate [1], [2]. To date, either lasers, light emitting diodes (LEDs), or micro LED arrays serve as photon emitters suitable for optical underwater communications. Subsequently, the focus will be on laser-based communication, which offers the highest range and the best signal-to-noise ratio among all optical transmitters due to beam collimation. Unlike LEDs, the phase can be utilized on both the transmitter and receiver sides. Furthermore, the bandwidth is significantly larger compared to any other alternative method. Compared to acoustic communication, the latency is considerably lower, and small as well as lightweight implementation is possible.

Manuscript received 20 July 2023; revised 3 September 2023; accepted 14 September 2023. Date of publication 19 September 2023; date of current version 28 September 2023. This work was supported by Land Schleswig-Holstein through Programme Open Access Publikationsfonds. *(Corresponding author: Ali Derakhshandeh.)*

Ali Derakhshandeh is with the Chair of Communications and the Chair of Information and Coding Theory, Kiel University, 24143 Kiel, Germany (e-mail: alid@tf.uni-kiel.de).

Stephan Pachnicke is with the Chair of Communications, Kiel University, 24143 Kiel, Germany (e-mail: stephan.pachnicke@tf.uni-kiel.de).

Peter A. Hoeher is with the Chair of Information and Coding Theory, Kiel University, 24143 Kiel, Germany (e-mail: ph@tf.uni-kiel.de).

Digital Object Identifier 10.1109/JPHOT.2023.3316729

Despite the advantages that optical communication offers, there are serious challenges to creating a reliable communication link particularly between moving vehicles. A line-of-sight (LOS) link is needed in laser-based wireless communication, which may not be strictly necessary for acoustic and RF communications. In addition, due to the very small aperture size of the transmitter and receiver, precise pointing at different angles is needed, as a slight misalignment can significantly impact communications performance and result in severe degradation or complete loss of the communications link. If the transceivers are not stationary, a tracking system for establishing a robust wireless laser communication link is vital. However, transceiver motion is not only associated with mobile stations, but also with temporary displacements of stationary terminals [3]. Pointing, acquisition, and tracking (PAT) techniques are critical to overcoming these challenges. The main goal of a PAT systems is to establish a LOS link. Pointing involves aligning the transmitter's laser beam with the receiver's field of view (FOV). Conversely, the receiver is aligned with the direction of the incoming beam during acquisition. Tracking plays an important role in maintaining alignment and acquisition by continuously tracking the position of the mobile transceiver so that data transmission can be kept stable [4].

In this paper, we consider three main challenges in underwater laser-based communication between moving vehicles: beam steering, beam widening, and scanning. We introduce a system concept based on optical phased array (OPA) antennas to electronically steer a laser beam in azimuth and elevation angles, and to simultaneously control the width of this laser beam. A wide beamwidth simplifies pointing and acquisition, while a narrow beamwidth maximizes the range of the communication link. To the best of our knowledge, we provide the first numerical evaluation of an underwater communication system using OPA technology. The novel approach of beam widening for the pointing and acquisition phase and beam narrowing for the communication phase is presented, which promises faster synchronization and higher throughput during communication. This innovative technique provides a highly effective solution for UOWC systems.

The remainder of the paper is organized as follows. Section II presents a brief review of different techniques commonly used for PAT in wireless laser communications, highlighting their pros and cons. Section III introduces the proposed system concept architecture. The configuration of the transmitter and receiver essential for the realization of the PAT system is detailed. Section IV discusses the beam divergence control

method suitable for the proposed system concept. In Section V, a scanning method appropriate for the case of wireless communication between autonomous underwater vehicles (AUVs) is examined. The justification for this choice and its potential benefits are discussed. Section VI features numerical results that evaluate the performance of the proposed system and demonstrate the effectiveness of the design. In Section VII conclusions are drawn.

II. Review of PAT and Beam Divergence Control Techniques

Various PAT systems have been developed and deployed for wireless optical communications, most of them for terrestrial or space applications. These techniques can be divided into three main categories: mechanical, electro-mechanical, and electronic beam steering techniques.

Mechanical PAT systems using a gimbal technique rely on a mechanically controlled rotating gimbal driven by motors. For example, a two-axis gimbal was used for long-range optical communications between balloons in [5]. This motor-driven system, to which a mirror is attached, allows active monitoring and alignment of the optical link through a two- or three-axis gimbal at both transmitter and receiver sides. This type of system is particularly well-suited for setups that require a large angular range. However, the heavy weight of gimbals, primarily due to the servo motors, makes them unsuitable for vehicles with strict weight restrictions [3], [4]. Another disadvantage of this approach is the low pointing resolution, which results in large angular steps, which is challenging especially at long ranges.

Electro-mechanical PAT systems use fast steering mirrors (FSMs), which result in a lighter system due to the lower mass of the mirrors and higher steering speed. For instance, in [6], a gimbal with two servo motors and connected FSMs is used for bidirectional air-to-air and air-to-ground communication, and in [7] for communication links between UAVs. However, electro-mechanical systems are still challenging because they offer only a limited range of angular motion. Another approach combines gimbals and FSMs to provide a wider range of angular motions but suffers from the problem of bulky equipment [3]. Mechanical as well as electro-mechanical techniques, the current standard in PAT for wireless laser-based communication links, possess several disadvantages. They tend to have a slow steering speed and lack beam agility. Furthermore, they are prone to vibrations and are bulky. The moving parts could lead to failure and consequently impact the reliability and precision of the system.

To address some of these problems, PAT systems based on OPAs are a promising alternative. OPAs offer significant advantages due to their high steering speed and the possibility of a small and lightweight implementation. In addition, the robustness and precision make OPAs a well-suited candidate for realizing wireless laser communication networks [8]. Even more important in our context, OPAs can be employed in free-space OWC as well as in UOWC applications. OPAs are based on the concept of optical interference, so they can steer the beam without any mechanical movement. This approach enables fast, accurate and reliable steering of the beam over large angles. However, this method comes with its own challenges, including design and manufacturing complexity and the need for high-speed electronic control.

In addition to PAT techniques, beam divergence control is an advantageous factor in wireless optical communications, impacting various performance metrics. Large beam divergence can facilitate PAT and tolerate alignment errors but simultaneously results in a higher path loss. On the other hand, a less divergent beam decreases the path loss but increases the scanning time and alignment error. In [9] a comparison of the narrow and wide laser beams in terms of received power, coverage area, and PAT complexity for free-space optical communications is investigated. One method is to use different lens groups, each group providing different divergence angles and an optical switch, which can switch between these lens groups [10]. Another approach is to use a lens and control the divergence angle by changing the relative position of the lens to the source. Recently other innovative techniques are introduced such as using variable focus lenses in [11], [12], [13]. In [12] three variable focus lenses (VFL) are employed, one on-axis lens for adaptive beam divergence control, and two off-axis lenses for PAT. VFLs are made of liquid lenses whose curvature can be adjusted by electro-wetting or pressure-driven elastic membranes. However, such mechanical techniques are prone to inaccuracy, and the speed of beam divergence control is limited. In contrast, electronic beam divergence control could offer more reliable and accurate solutions. According to [14], in RF phased arrays, beam shaping methods are based on changing the amplitude factor of each antenna element. In optical phased arrays, the implementation of nonuniform antenna arrays is challenging, primarily due to the difficulties in allocating varying intensities to different paths using conventional optical splitters. An alternative could involve variable optical splitters (VOS), which allow for controlled splitting ratios [15], [16]. VOSs give the possibility to control the weighting factor of each antenna element. However, this approach introduces further complexity in controlling the splitting ratio and incurs higher loss compared to conventional optical splitters. An innovative approach to beam divergence control without altering the amplitude factor of each antenna element has been introduced in [17]. This method relies on dividing the antenna array into multiple subarrays. Building upon this innovative approach, our study also employs the strategy of dividing the antenna array into multiple subarrays to effectively control the beam divergence.

III. Proposed System Concept Architecture

The general configuration of the transmitter and receiver system concept for point-to-point communication is shown in Fig. 1. The system concept supports bi-directional communication between underwater vehicles, in which their transceivers are not aligned along the same axis. The beam steering is based on optical phased array technology. The main advantage of adopting phased array technology for optical beam steering is the avoidance of large, imprecise mechanical components,

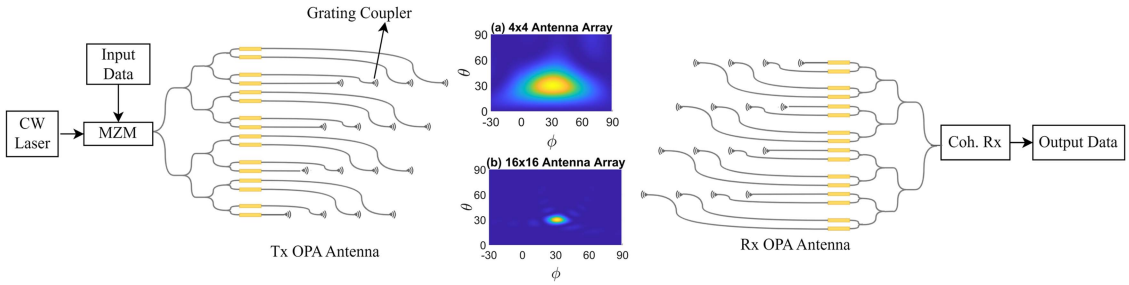

Fig. 1. System concept architecture of a laser-based wireless communication system using OPA antennas. (a) Directivity of the OPA system with (4×4) antenna elements. (b) Directivity of the OPA system with (16x16) antenna elements, adjusted to steer the laser beam at the desired direction $(\theta_0, \phi_0) = (30°, 30°)$.

especially in communication applications where pointing accuracy is a direct indicator of communication performance.

A continuous-wave (CW) laser is chosen as the light source. An IQ-Mach-Zehnder-Modulator (MZM) is used for complex-valued modulation. We assume a photonics integrated circuit (PIC) on a silicon waveguide for the OPA antenna as suggested in [18]. The transceiver OPA antenna includes 3 dB splitters, phase shifters, and grating couplers. Silicon nitride waveguides and splitters are transparent for light in the wavelength region from about 400 nm to 2350 nm. The propagation losses in waveguides for $\lambda = 500$ nm are typically around 0.3-0.4 dB/cm, and the splitters have an insertion loss of roughly 0.1 dB [19], [20]. All the photonics components used in our system concept such as MZM, splitters, phase shifters, and grating couplers are implementable in the 500 nm wavelength region. A phase shifter changes the refractive index of the silicon waveguide, resulting in a phase shift of the light. This creates a phase gradient throughout the waveguide array, which allows beam steering. Grating couplers are then used to couple the light out of the waveguide after phase adjustment. On the other hand, grating couplers are employed at the receiver side to couple the light into the waveguides. Additionally, the splitters serve as combiners [18], [21]. A 2D array of photonics antenna elements are arranged uniformly on a planar surface to create the transceiver aperture.

The theoretical background of optical phased arrays is the same as microwave phased arrays [14]. The fundamental distinction between OPA and microwave phased arrays is the optical wavelength. This influences the system design, including power transfer and receiver sensitivity, and defines the size and spacing of the antennas. The theory can be well explained based on Fraunhofer's diffraction theory. The phase of each antenna element is controlled to achieve a specific desired far-field radiation pattern. The far field is the sum of all fields radiated from each antenna element and can be written as [14]

$$E(\theta,\phi) = \sum_{n=1}^{N}\sum_{m=1}^{M} E_{n,m}(\theta,\phi) = \int_0^{2\pi}\int_0^{\pi} AF(\theta_0,\phi_0)\, E_i(\theta,\phi)\, d\theta\, d\phi. \quad (1)$$

$AF(\theta_0, \phi_0)$ is the array factor for the desired angle (θ_0, ϕ_0), and $E_i(\theta, \phi)$ is the transmitted field by a single antenna element. As in radar theory, by manipulating the phase of the antenna elements most of the laser beam can be radiated in the desired angle (θ_0, ϕ_0). The array factor in the two-dimensional case can be written as [14]

$$AF(\theta_0,\phi_0) = \sum_{n=1}^{N} e^{jkd_x(n-1)(\sin\theta\cos\phi-\beta_x)} \cdot \sum_{m=1}^{M} e^{jkd_y(m-1)(\sin\theta\sin\phi-\beta_y)}, \quad (2)$$

where $\beta_x = \sin\theta_0\cos\phi_0$, $\beta_y = \sin\theta_0\sin\phi_0$, $d_{x/y}$ are the distance, and $\beta_{x/y}$ the phase shifts between the antenna elements in x/y directions, respectively. More details about the array factor can be found in [14].

The same architecture as at the transmitter with the same mathematical principle is also applied at the receiver side. The selective directivity of the OPA receiver enables spatially selective reception, reducing channel interference and enhancing system reliability while filtering out undesirable light from other directions. Through electronically controllable on-chip processing, the system functions as an adaptive lens, allowing the chip to replicate the conventional lens functions, like any shape and orientation [22].

A measure of the performance of the radiation is the directivity $D(\theta, \phi)$ of the antenna array. Directivity is the ratio of the radiation intensity from the antenna in a given direction over the radiation intensity averaged across all directions, which determines the transceiver gain [14], and can be written as

$$D(\theta,\phi) = \frac{4\pi\, I(\theta,\phi)}{P_{\text{rad}}} = \frac{1}{\eta}\, G(\theta,\phi) = \frac{4\pi\,[AF]\,[AF]^*}{\int_0^{2\pi}\int_0^{\pi}[AF]\,[AF]^*\sin\theta\, d\theta\, d\phi}, \quad (3)$$

where $I(\theta, \phi)$ is the radiation intensity of the OPA, and P_{rad} is the total radiated power. Knowing the directivity, the Friis formula can be used to determine the link budget in air as follows:

$$P_{r,\text{air}} = P_t\, \eta_{\text{MZM}}\, \eta_t\, D_t\, \eta_r\, D_r \left(\frac{\lambda}{4\pi R}\right)^2. \quad (4)$$

P_t and P_r are the transmit and received power respectively, η_{MZM} is the MZM efficiency, D_t and D_r are the transmitter and

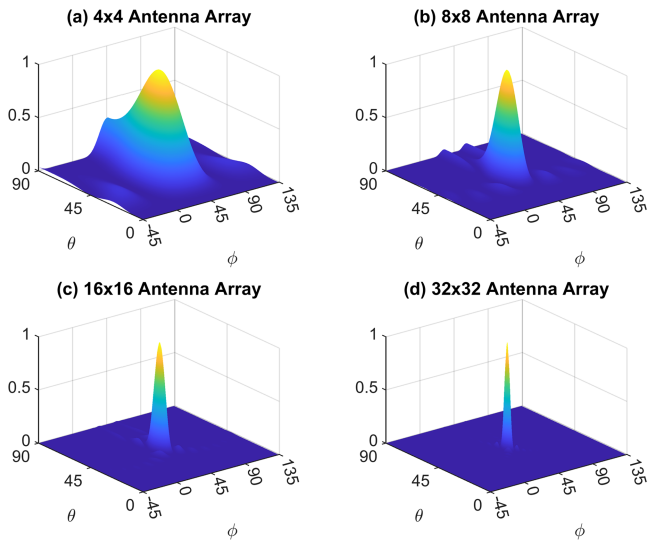

Fig. 2. Normalized directivity for different numbers of antenna elements, optimized to radiate at $(\theta_0, \phi_0) = (45°, 45°)$.

TABLE I
BEAMWIDTH AND DIRECTIVITY FOR DIFFERENT NUMBERS OF ANTENNA ELEMENTS

Number of antenna elements	$\Delta\theta_{10\,\mathrm{dB}}$	$\Delta\phi_{10\,\mathrm{dB}}$	Directivity
2×2	90.00°	87.00°	10.22 dB
4×4	72.25°	64.00°	16.52 dB
8×8	34.12°	32.00°	22.75 dB
16×16	16.12°	15.00°	28.90 dB
32×32	7.87°	7.00°	34.99 dB

receiver directivity, and η_t and η_r are constants, which express the antenna efficiency. The term $(\frac{\lambda}{4\pi R})^2$ corresponds to the path loss of a spherical wave that has traveled a distance R in air. The directivity depends highly on the number of antenna elements.

In Fig. 2 the directivities of antennas with four different element numbers are shown, which are optimized to radiate at $(\theta_0, \phi_0) = (45°, 45°)$. As it is obvious from Fig. 2, the higher the number of antenna elements, the narrower the laser beam gets. Let us define the beamwidth as the section of the beam where the radiation intensity $I(\theta, \phi)$ remains within 10 dB of its maximum value. In Table I, the beamwidth, as a function of θ and ϕ together with the corresponding directivity is calculated using (3) for different numbers of antenna elements. This table confirms the previously made argument: As the number of antenna elements increases, the beam width narrows, which leads to a higher directivity.

IV. BEAM DIVERGENCE CONTROL

The system concept, as previously mentioned, is based on two-dimensional optical phased arrays. The phase shift for each antenna element is determined based on the desired radiation angle. Consequently, the achieved beamwidth and directivity are dependent upon the number of antenna elements. Crucial to our discussion is the control of beam divergence, which is essential for fulfilling various task requirements such as scanning, acquisition, and communication. Notably, in the scanning method outlined in the subsequent section, beam divergence control is crucial to simplify and speed up the scanning process. The basic theory of beam broadening is built upon amplitude variations. However, in optical phased arrays implemented in photonics integrated circuits (PICs), assigning different amplitudes to each waveguide increases system complexity. In [17] an approach for beam broadening is proposed that involves subdividing the antenna array into subarrays. The beam divergence control for our system concept follows this approach. By allocating different neighboring angles of the desired angle of radiation (θ_0, ϕ_0) for the beamforming of each array group, we achieve broader beams compared to the case that the beamforming is optimized to steer the beam to (θ_0, ϕ_0) for all antenna elements. The array factor in (2) can be written as:

$$AF(\theta, \phi) = \sum_{g=1}^{G} AF(\theta_0 + \Delta\theta_g, \phi_0 + \Delta\phi_g), \tag{5}$$

where G is the number of subarrays and $\Delta\theta$, and $\Delta\phi$ are the angular displacement of the desired radiation between each subarray. Each subarray radiates a beam, which covers the region around its defined desired angle. Equation (5) shows that the radiated beam is a result of the superposition of all individual beams. Importantly, the beamwidth of this beam is constrained by the beamwidths of all individual beams:

$$(\Delta\theta_{10\,\mathrm{dB}}, \Delta\phi_{10\,\mathrm{dB}}) \leq \bigcup_{g=1}^{G} (\Delta\theta_{10\,\mathrm{dB}}, \Delta\phi_{10\,\mathrm{dB}})_g \tag{6}$$

By manipulating the angular displacement we can control the beam divergence angle. In Figs. 3 and 4 a (32×32) antenna array is divided into four (16×16) subarrays. By increasing $\Delta\phi$ the beamwidth increases. The lower limit is the beamwidth of one subarray, and the upper limit is the sum of the beamwidths. If the $\Delta\phi$ increases further, some fluctuations of intensity occur and the separation of the beams becomes visible as it is shown in Fig. 4(d), and a united beam cannot be achieved anymore.

In order to have a symmetrical and almost round-shaped beam, the neighboring angles are chosen equiangular around the desired angle as shown in Fig 5. As mentioned before, if the angular displacement is higher than the upper limit, the beam separation is visible as shown in Fig. 4(d).

V. PROPOSED SCANNING METHOD

The establishment of a successful communication link depends on two essential conditions. The first condition is that the transmitted beam should hit the aperture of the receiver. The second condition is that the angle of the incoming beam has to be within the receiver's FOV, which determines the maximum allowed angle for the incoming beam. Even if the incoming beam reaches the aperture of the receiver, it must be within the receiver's FOV to be successfully coupled into the receiving antenna [23]. To satisfy these conditions, the initialization phase of the PAT algorithm requires a scanning algorithm for position estimation. Both the transmitter and receiver are tasked with

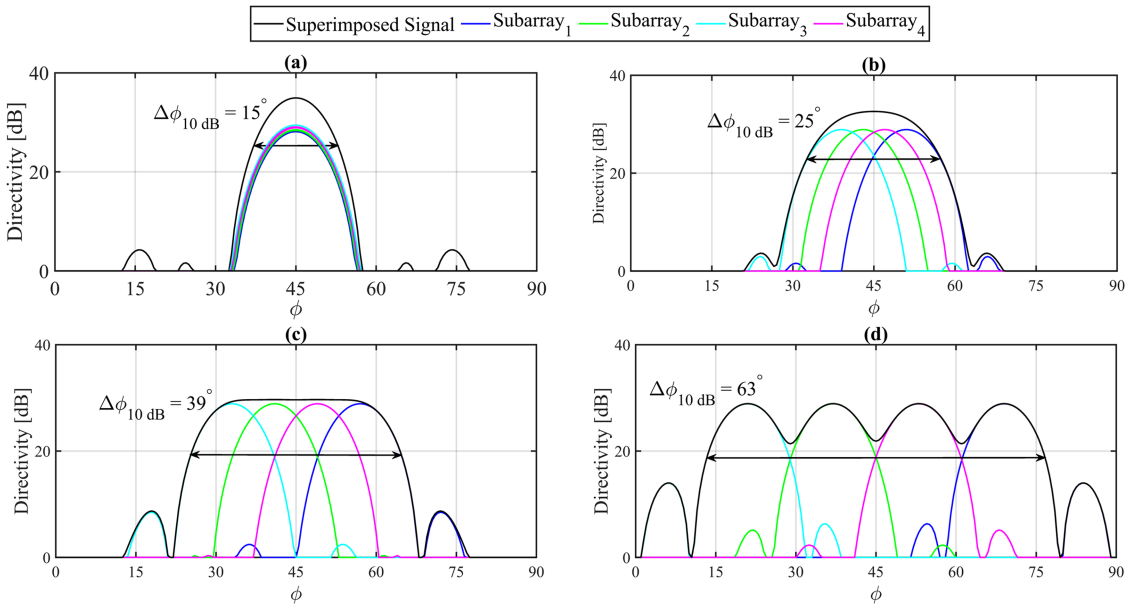

Fig. 3. Beam broadening method in ϕ with different angular displacements $\Delta\phi$. The black arrows show the beamwidth. (a) $\Delta\phi = 0^\circ$, $\Delta\phi_{10\,\mathrm{dB}} = 15^\circ$ (b) $\Delta\phi = 4^\circ$, $\Delta\phi_{10\,\mathrm{dB}} = 25^\circ$, (c) $\Delta\phi = 8^\circ$, $\Delta\phi_{10\,\mathrm{dB}} = 39^\circ$, (d) $\Delta\phi = 16^\circ$, $\Delta\phi_{10\,\mathrm{dB}} = 63^\circ$.

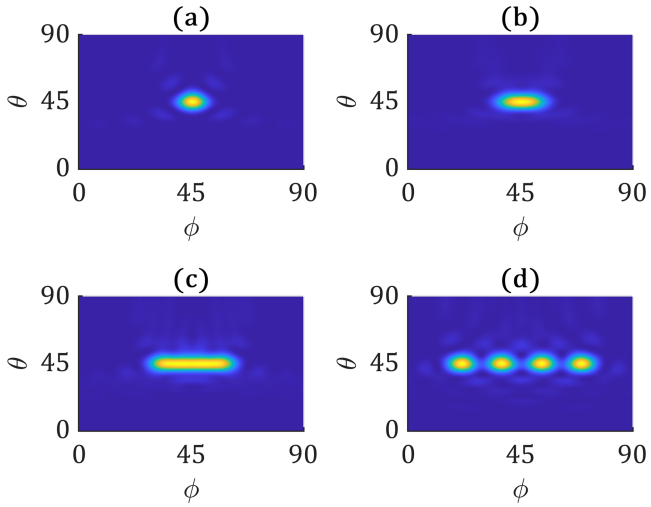

Fig. 4. Beam intensities for different angular displacements $\Delta\phi$. (a) $\Delta\phi = 0^\circ$, (b) $\Delta\phi = 4^\circ$, (c) $\Delta\phi = 8^\circ$, (d) $\Delta\phi = 16^\circ$, .

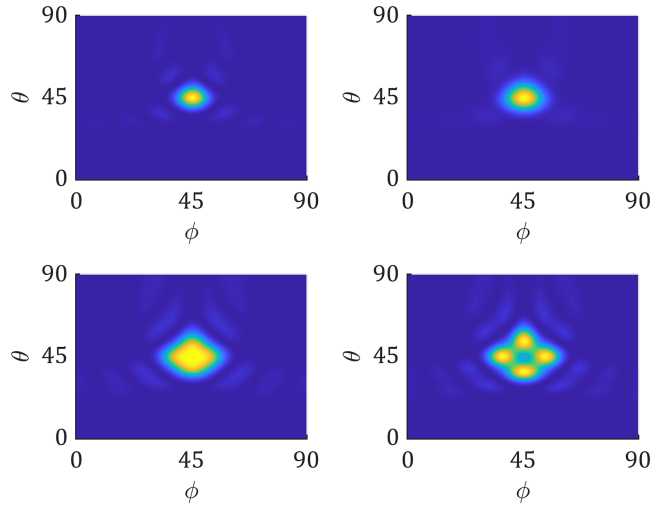

Fig. 5. Beam broadening in two dimensions θ and ϕ.

scanning a specific subspace, also known as the uncertainty cone. In this cone, the exact locations of the transmitters and receivers are unknown due to spatial uncertainties [24]. An Archimedean spiral-based scanning algorithm can be employed for this task. The spiral is defined by three parameters: The number of rotations in the uncertainty cone ω_0, the radius of the cone r_0, and the duration of the scan from the origin to the border of the cone t_0, and can be written as [25]

$$x(t) = \frac{r_0}{t_0}\, t\, \cos\left(2\pi\, \frac{\omega_0}{t_0}\, t\right)$$
$$y(t) = \frac{r_0}{t_0}\, t\, \sin\left(2\pi\, \frac{\omega_0}{t_0}\, t\right). \qquad (7)$$

The scan starts at the coordinate origin and rotates within the uncertainty cone until the maximum predefined scanning angle, corresponding to r_0 is reached, which also marks the boundary of the uncertainty cone. It is reasonable to assume a Gaussian probability distribution for the position of the transceiver within this uncertainty cone. This assumption emphasizes the appropriateness of the Archimedean spiral algorithm for scanning, particularly due to the fact that it initiates its search at the center of the uncertainty cone - the most probable location of the receiver according to the Gaussian distribution. The scanning time t_0 depends on the number of scanning points, which depends on the size of the uncertainty cone and the scanning beam's size to cover the whole area as shown in Fig. 6. Once

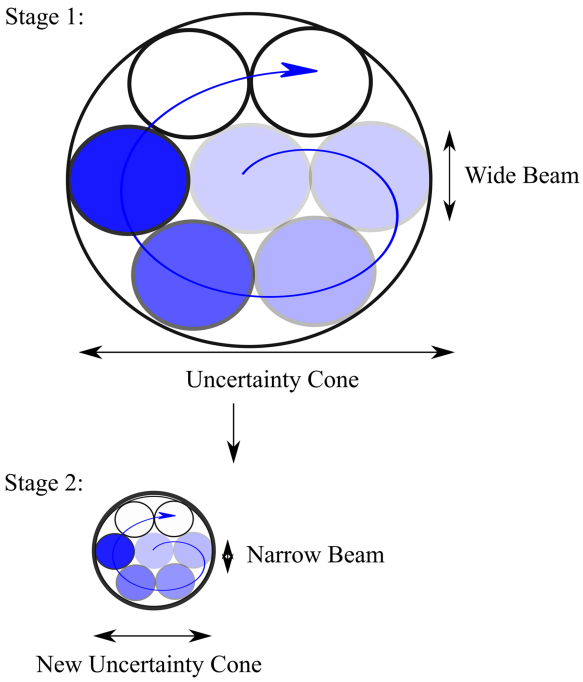

Fig. 6. Proposed scanning method. In stage 1 the transmitter scans with a wide beam in the uncertainty cone from the center. After finding the approximate position of the receiver, the uncertainty cone gets smaller, and a narrower beam scans in the new uncertainty cone in stage 2.

the scanning beam successfully reaches the receiver, localization should occur. There are two methods for determining the relative positions of both communication endpoints. The first involves transmitting the rotational information of each point scanning point in the Archimedean spiral. However, this method may face potential limitations, as the receiver might not recover this information due to the wide laser beam and possibly diminished signal power during the scanning phase, which could fall below the FEC threshold. An alternative method involves extracting the angular information of the steered receiving antenna at coordinates (θ_0, ϕ_0), where maximum intensity is received. The combination of this intrinsic and extrinsic information on the receiver side could provide higher reliability. As mentioned before, minor misalignments can significantly degrade communication performance. Therefore, for accurate pointing, it is critical to refine the alignment in different steps. This need arises not only to enhance the pointing accuracy but also to optimize the scanning process: commencing with a narrow beam during the initial scanning phase could yield an excessive number of scanning points within the uncertainty cone, thus prolonging the scanning time. In response to this issue, our proposed system concept supports efficient scanning while enhancing pointing accuracy to avoid misalignment. The process is initiated with a broader beamwidth at the transmitter side and a larger FOV on the receiver end. This approach facilitates covering the uncertainty cone with fewer points. Once the scanning beam is in the LOS of the receiver, and the acknowledgment signal is sent, the uncertainty cone is reduced to the size of the scanning beamwidth. Subsequently, the scanning beamwidth and the FOV at the receiver are reduced. Scanning is then performed within the new smaller uncertainty cone. These steps are repeated until the narrowest possible laser beamwidth and FOV, and hence the highest possible gains at both ends are achieved. Ultimately, the handshake is possible, and the bi-directional communication along with the tracking phase can begin.

Both the beam divergence and the scanning method are controlled by changing the phase shifters' array. The electronic control unit can be a field-programmable gate array (FPGA) or a microcontroller, depending on the required scanning speed.

Implementing optical phased arrays in silicon photonic integrated circuits presents several challenges. A major issue is the spacing between the grating couplers, which serve as the antenna elements in the phased array. In the antenna array, the spacing should be half of the wavelength $(\lambda/2)$ to prevent grating lobes, translating to $\lambda/2 = 250\,\text{nm}$ in our proposed system concept. This requires advanced techniques such as e-beam lithography. Moreover, it is vital to ensure proper spacing between waveguides to prevent crosstalk and unwanted coupling.

The control mechanism of the phase shifter is very similar to the control of an MZM and it does not require any sophisticated computational complexity. To reduce the computational complexity, we can pre-calculate and store the phase distribution of the elements and create a look-up table (LUT) for beamforming.

VI. Numerical Results

A. Channel Model

The major factors impacting UOWC are absorption, scattering, beam spreading, turbulence, alignment, multipath interference, physical obstruction, and background noise [26]. In any underwater optical communications link signal attenuation due to absorption and scattering is by far the most significant loss factor [27]. The most frequently used channel model for underwater optical propagation is based on the Lambert law. This model considers absorption and scattering effects, which are the two factors that contribute to attenuation. Turbulence causes variations of the refractive index along the propagation path due to density, salinity, and temperature fluctuations. Turbulence can cause large variations in the intensity of the signal at the receiver, which is called scintillation [26]. A channel model considering absorption, scattering, and turbulence should be modeled stochastically based on PDFs, because of the random variations in turbulence. BER predictions can be done by Monte Carlo simulations [28], besides experiments. Adaptive optics can compensate to some extent for the effects of turbulence [29]. The influence of turbulence on the OPA-based system is an interesting research topic for future work. So far we did not consider turbulence in our model.

The underwater optical attenuation coefficient $c(\lambda)$ is defined by two inherent optical properties of water, absorption $a(\lambda)$, and scattering $b(\lambda)$, which can be written as $c(\lambda) = a(\lambda) + b(\lambda)$. Parameter c is not to be confused with the speed of light. The light attenuation after traveling the distance R in water, with the transmit power P_t can be calculated by Beer-Lambert's law:

$$P_{r,\text{water}} = P_t\, \eta_{\text{MZM}}\, \eta_t\, D_t\, \eta_r\, D_r \left(\frac{\lambda}{4\pi R}\right)^2 e^{-c(\lambda)\cdot R}. \quad (8)$$

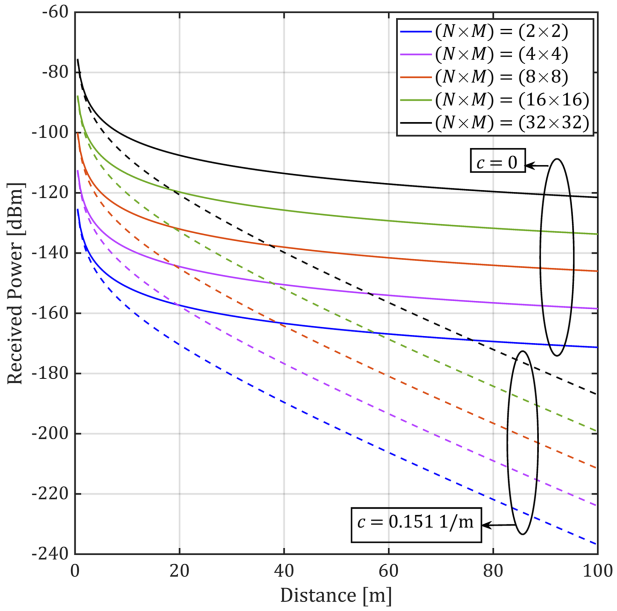

Fig. 7. Received power vs. distance for different numbers of antenna elements, in **free space** (solid lines), and **clean ocean** (dashed lines).

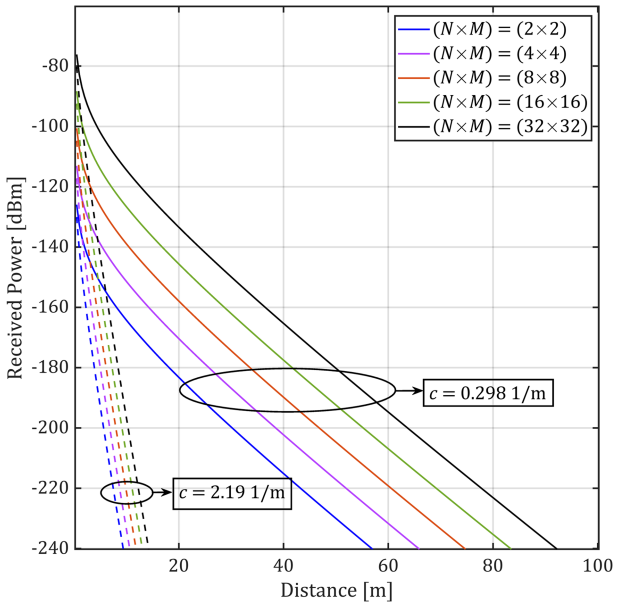

Fig. 8. Received power vs. distance for different numbers of antenna elements, in **coastal ocean** (solid lines), and **turbid harbor** (dashed lines).

The resulting received power for different channels as a function of distance is shown in Figs. 7 and 8. The attenuation of the transmit optical signal depends directly on the amount of water volume it interacts with. A smaller volume of water interaction leads to reduced attenuation [30]. In the proposed system concept, it is possible to narrow the laser beam. This narrowing, which is related to the increase in the number of antenna elements, results in lower attenuation, as can be clearly seen in Figs. 7 and 8. In the numerical results, typical attenuation coefficients for clean ocean, coastal ocean, and turbid harbor are considered, as reported in [31].

TABLE II
PARAMETERS USED FOR NUMERICAL SIMULATIONS

Parameter	Value
Carrier frequency	$f_c = 600\,\mathrm{THz}$
Atten. coeff. in pure sea water	$c = 0.043\,1/\mathrm{m}$
Atten. coeff. in clean ocean	$c = 0.151\,1/\mathrm{m}$
Atten. coeff. in coastal ocean	$c = 0.298\,1/\mathrm{m}$
Atten. coeff. in turbid harbor	$c = 2.19\,1/\mathrm{m}$
Signal bandwidth	$B = 1\,\mathrm{GHz}$
Laser launch power	$P_t = 10\,\mathrm{mW}\,(10\,\mathrm{dBm})$
Efficiency of MZM	$\eta_{\mathrm{MZM}} = 31.6\,\%\,(-5\,\mathrm{dB})$
Efficiency of Tx OPA	$\eta_t = 50\,\%\,(-3\,\mathrm{dB})$
Efficiency of Rx OPA	$\eta_r = 50\,\%\,(-3\,\mathrm{dB})$

B. Performance Evaluation

In order to be able to evaluate the potential performance of the system concept, we have made assumptions based on proven and tested devices. This ensures our evaluations are rooted in proven and tested devices. The efficiency considerations in the simulation are based on rough estimations based on measurements in already implemented OPAs [22], [32], [33], and also calculations based on the losses of the photonics elements in PICs at the 500 nm wavelength region. Parameter values were selected according to Table II. A CW laser with a carrier frequency of 600 THz (i.e. $\lambda = 500$ nm in air) is chosen as the source. The transceiver efficiency is assigned a value of 50% each, as indicated in [34], while the MZM efficiency is set to 31.6%.

The relation between the maximum achievable data rate R_b and the signal-to-noise ratio (SNR) measured at the detector input can be expressed by [35]

$$R_\mathrm{b} = B\,\log_2(1+\mathrm{SNR}), \tag{9}$$

where B denotes the signal bandwidth. Noise is caused by shot noise and thermal noise, among other noise sources. Assuming binary phase shift keying modulation, the BER can be calculated as [36]

$$\mathrm{BER} = \frac{1}{2}\,\mathrm{erfc}\sqrt{\mathrm{SNR}}. \tag{10}$$

Given (9) and (10) and for a given channel-dependent distance law, an upper bound on the distance can be established as a function of a target BER. In the numerical results presented next, typical SNR values are taken from measurements reported in [22].

As mentioned before, different water types have different attenuation coefficients. As a reference, in Fig. 9(a) the achievable data rate and BER for four different numbers of antenna elements in free space are shown, and in Fig. 9(b), (c), and (d) three water types, i.e. pure sea water, clean ocean and, coastal ocean, are shown. The simulation results for turbid harbor indicate that the communication range is less than 5 m. These curves give us an upper bound on the data rate and BER that can be achieved by OPA-based underwater communications systems. Additionally, the figures highlight the trade-offs between data rate and communication distance. No channel coding scheme

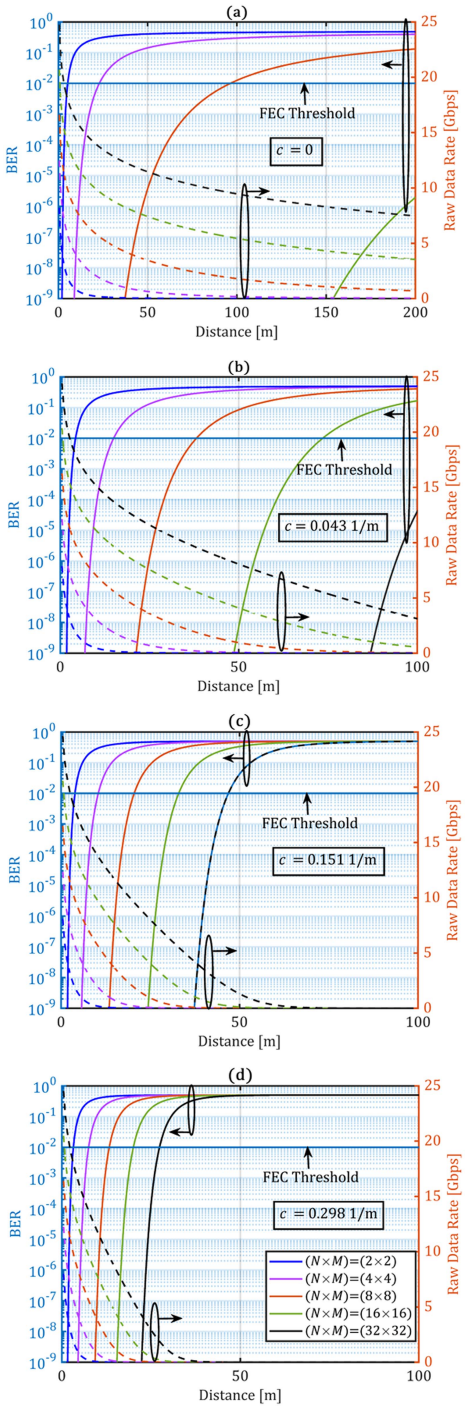

Fig. 9. BER and data rate analysis for different numbers of antenna elements, (blue: (2×2), magenta: (4×4), red: (8×8), green: (16×16), black: (32×32)), in (a) **free space** ($c = 0$), (b) **pure sea water** ($c = 0.043\,1/m$), (c) **clean ocean** ($c = 0.151\,1/m$), and (d) **coastal ocean** ($c = 0.298\,1/m$).

is used in the performance evaluation. A soft-decision forward error correction (SD-FEC) code with $15.8\&percnt$; overhead can achieve an FEC threshold of $1.25 \cdot 10^{-2}$. On that basis, the communication link can support a range of up to 120 meters in pure sea water, 46 meters in clean ocean, and 27 meters in coastal ocean with an achievable raw data rate of 1.8 Gbps assuming a launch power of 10 mW. Comparing the results in Fig. 9, it becomes clear that the optimum operating range for the communication system is significantly influenced by the type of water.

VII. Conclusion

In this paper, an optical phased array-based electronically steerable laser beam is proposed for underwater laser communication. The proposed approach allows control of the laser beamwidth for acquisition and communication phases and promises faster synchronization and higher throughput communication. On the receiver side, the system concept offers the advantage of spatially selective reception, which reduces interference and increases receiver gain. Simulation results show potential for improving underwater communications in terms of range and throughput between non-aligned transceivers. In future work, experimental verification is targeted.

References

[1] Z. Zeng, S. Fu, H. Zhang, Y. Dong, and J. Cheng, "A survey of underwater optical wireless communications," *IEEE Commun. Surveys Tut.*, vol. 19, no. 1, pp. 204–238, Firstquarter 2017.

[2] P. A. Hoeher, J. Sticklus, and A. Harlakin, "Underwater optical wireless communications in swarm robotics: A tutorial," *IEEE Commun. Surveys Tut.*, vol. 23, no. 4, pp. 2630–2659, Fourthquarter 2021.

[3] Y. Kaymak, R. Rojas-Cessa, J. Feng, N. Ansari, M. Zhou, and T. Zhang, "A survey on acquisition, tracking, and pointing mechanisms for mobile free-space optical communications," *IEEE Commun. Surveys Tut.*, vol. 20, no. 2, pp. 1104–1123, Secondquarter 2018.

[4] R. Abdelfatah, N. Alshaer, and T. Ismail, "A review on pointing, acquisition, and tracking approaches in UAV-based FSO communication systems," *Opt. Quantum Electron.*, vol. 54, no. 9, 2022, Art. no. 571.

[5] B. Moision et al., "Demonstration of free-space optical communication for long-range data links between balloons on project loon," *Proc. SPIE*, vol. 10096, pp. 259–272, 2017.

[6] A. G. Talmor, H. Harding Jr., and C.-C. Chen, "Two-axis gimbal for air-to-air and air-to-ground laser communications," *Proc. SPIE*, vol. 9739, pp. 129–135, 2016.

[7] C. Chen et al., "High-speed optical links for UAV applications," *Proc. SPIE*, vol. 10096, pp. 316–324, 2017.

[8] J. He, T. Dong, and Y. Xu, "Review of photonic integrated optical phased arrays for space optical communication," *IEEE Access*, vol. 8, pp. 188284–188298, 2020.

[9] Y. Kaymak, R. Rojas-Cessa, J. Feng, N. Ansari, and M. Zhou, "On divergence-angle efficiency of a laser beam in free-space optical communications for high-speed trains," *IEEE Trans. Veh. Technol.*, vol. 66, no. 9, pp. 7677–7687, Sep. 2017.

[10] K. H. Heng, W.-D. Zhong, T. H. Cheng, N. Liu, and Y. He, "Beam divergence changing mechanism for short-range inter-unmanned aerial vehicle optical communications," *Appl. Opt.*, vol. 48, no. 8, pp. 1565–1572, 2009.

[11] M. Zohrabi, R. H. Cormack, and J. T. Gopinath, "Wide-angle nonmechanical beam steering using liquid lenses," *Opt. Exp.*, vol. 24, no. 21, pp. 23798–23809, 2016.

[12] V. V. Mai and H. Kim, "Non-mechanical beam steering and adaptive beam control using variable focus lenses for free-space optical communications," *J. Lightw. Technol.*, vol. 39, no. 24, pp. 7600–7608, Dec. 2021.

[13] K. Lee, V. Mai, and H. Kim, "Dynamic adaptive beam control system using variable focus lenses for laser inter-satellite link," *IEEE Photon. J.*, vol. 14, no. 4, Aug. 2022, Art. no. 7337108.

[14] C. A. Balanis, *Antenna Theory: Analysis and Design*. Hoboken, NJ, USA: Wiley, 2015.

[15] N. Gogoi and P. P. Sahu, "All-optical tunable power splitter based on a surface plasmonic two-mode interference waveguide," *Appl. Opt.*, vol. 57, no. 10, pp. 2715–2719, 2018.

[16] S. Liao, H. Bao, T. Zhang, J. Liu, X. Liao, and L. Liu, "Integrated optical power splitter with continuously adjustable power splitting ratio," *IEEE Photon. J.*, vol. 12, no. 6, Dec. 2020, Art. no. 7801513.

[17] S. Rajagopal, "Beam broadening for phased antenna arrays using multi-beam subarrays," in *Proc. IEEE Int. Conf. Commun.*, 2012, pp. 3637–3642.

[18] Y. Guo, Y. Guo, C. Li, H. Zhang, X. Zhou, and L. Zhang, "Integrated optical phased arrays for beam forming and steering," *Appl. Sci.*, vol. 11, no. 9, 2021, Art. no. 4017.

[19] T. A. Huffman, G. M. Brodnik, C. Pinho, S. Gundavarapu, D. Baney, and D. J. Blumenthal, "Integrated resonators in an ultralow loss Si_3N_4/SiO_2 platform for multifunction applications," *IEEE J. Sel. Topics Quantum Electron.*, vol. 24, no. 4, Jul./Aug. 2018, Art. no. 5900209.

[20] D. J. Blumenthal, R. Heideman, D. Geuzebroek, A. Leinse, and C. Roeloffzen, "Silicon nitride in silicon photonics," *Proc. IEEE*, vol. 106, no. 12, pp. 2209–2231, Dec. 2018.

[21] C.-P. Hsu et al., "A review and perspective on optical phased array for automotive LiDAR," *IEEE J. Sel. Topics Quantum Electron.*, vol. 27, no. 1, Jan./Feb. 2021, Art. no. 8300416.

[22] R. Fatemi, B. Abiri, A. Khachaturian, and A. Hajimiri, "High sensitivity active flat optics optical phased array receiver with a two-dimensional aperture," *Opt. Exp.*, vol. 26, no. 23, pp. 29983–29999, 2018.

[23] T.-H. Ho, S. Trisno, I. I. Smolyaninov, S. D. Milner, and C. C. Davis, "Studies of pointing, acquisition, and tracking of agile optical wireless transceivers for free-space optical communication networks," *Proc. SPIE*, vol. 5237, pp. 147–158, 2004.

[24] C. Xu, T. Yang, and E. Rojas, "Agile beaconless laser beam alignment with adaptive mm-Wave beamforming for inter CubeSat communication," in *Proc. IEEE Int. Conf. Space Opt. Syst. Appl.*, 2022, pp. 218–223.

[25] T. T. Nguyen, A. Amthor, and C. Ament, "High precision laser tracker system for contactless position measurement," in *Proc. IEEE Int. Conf. Control Syst., Comput. Eng.*, 2011, pp. 97–102.

[26] H. Kaushal and G. Kaddoum, "Underwater optical wireless communication," *IEEE Access*, vol. 4, pp. 1518–1547, 2016.

[27] A. S. Fletcher, S. A. Hamilton, and J. D. Moores, "Undersea laser communication with narrow beams," *IEEE Commun. Mag.*, vol. 53, no. 11, pp. 49–55, Nov. 2015.

[28] W. Liu, Z. Xu, and L. Yang, "SIMO detection schemes for underwater optical wireless communication under turbulence," *Photon. Res.*, vol. 3, no. 3, pp. 48–53, 2015.

[29] I. Toselli and S. Gladysz, "Improving system performance by using adaptive optics and aperture averaging for laser communications in oceanic turbulence," *Opt. Exp.*, vol. 28, no. 12, pp. 17347–17361, 2020.

[30] S. A. Hamilton et al., "Undersea narrow-beam optical communications field demonstration," *Proc. SPIE*, vol. 10186, pp. 7–22, 2017.

[31] C. Mobley, *Light and Water*. New York, NY, USA: Academic Press, 1994.

[32] K. V. Acoleyen, R. Baets, and H. Rogier, "Chip-to-chip optical wireless link feasibility using optical phased arrays on silicon-on-insulator," in *Proc. IEEE 7th Int. Conf. Group IV Photon.*, 2010, pp. 243–245.

[33] K. Van Acoleyen, H. Rogier, and R. Baets, "Feasibility study of integrated optical phased arrays for indoor Gb/s wireless optical links," in *Proc. IEEE 35th Eur. Conf. Opt. Commun.*, 2009, pp. 1–2.

[34] K. V. Acoleyen, H. Rogier, and R. Baets, "Two-dimensional optical phased array antenna on silicon-on-insulator," *Opt. Exp.*, vol. 18, no. 13, pp. 13655–13660, 2010.

[35] C. E. Shannon, "A mathematical theory of communication," *Bell Syst. Tech. J.*, vol. 27, no. 3, pp. 379–423, 1948.

[36] J. G. Proakis, *Digital Communications*, 5th ed. New York, NY, USA: McGraw-Hill, 2008.